

Proceeding Paper

Nonlinear Control Design of Three-Level NPC-Based HVDC Systems for Enhanced Availability during AC Faults with Semi-Experimental Validation [†]

Ilyass El Myasse ^{1,*} , Aziz Watil ¹, Abdelmounime El Magri ¹ and Ambe Harrison ²

¹ EEIS Laboratory, ENSET Mohammedia, Hassan II University of Casablanca, Morocco; azizwatil@gmail.com (A.W.); magri_mounaim@yahoo.fr (A.E.M.)

² Department of Electrical and Electronics Engineering, College of Technology (COT), University of Buea, P.O. Box Buea 63, Cameroon; ambe.harrison@ubuea.cm

* Correspondence: ilyaselmyasse@gmail.com or ilyass.elmyasse-etu@etu.univh2c.ma

[†] Presented at the 4th International Electronic Conference on Applied Sciences, 27 October–10 November 2023; Available online: <https://asec2023.sciforum.net/>.

Abstract: This research paper addresses the issue of enhancing the operational availability of NPC three-level converter-based high voltage direct current (HVDC) transport systems during alternating current (AC) grid fault conditions. During short-circuit faults in power transmission lines, voltage sags can occur, causing fluctuations in the DC link voltage of converter systems. These voltage sags have the potential to induce reversed power flow and lead to the tripping of VSC-HVDC transmission systems. The objective of this paper is to develop a nonlinear control technique that investigates the fault ride-through (FRT) capability of VSC-HVDC transmission system characteristics during voltage sag events. To achieve this, we conduct semi-experimental investigations using Processor-in-the-loop (PIL) simulations and analyze the results. Symmetrical and asymmetrical voltage sag events with different remaining voltages are applied to an AC grid, and their effects are observed for varying durations. The proposed nonlinear control technique aims to mitigate the impact of voltage sags on the operational availability of HVDC transport systems. By analyzing the semi-experimental results, we aim to gain insights into the FRT capability of the VSC-HVDC transmission system.

Keywords: high voltage direct current; NPC three-level converter; voltage sags; AC fault; Backstepping technique



Citation: Myasse, I.E.; Watil, A.; Magri, A.E.; Harrison, A. Nonlinear Control Design of Three-Level NPC-Based HVDC Systems for Enhanced Availability during AC Faults with Semi-Experimental Validation. *Eng. Proc.* **2023**, *52*, 0. <https://doi.org/>

Academic Editor: Andrea Ballo

Published:



Copyright: © 2023 by the authors. Licensee MDPI, Basel, Switzerland. This article is an open access article distributed under the terms and conditions of the Creative Commons Attribution (CC BY) license (<https://creativecommons.org/licenses/by/4.0/>).

1. Introduction

In modern electrical power transmission, High Voltage Direct Current (HVDC) systems have emerged as vital components of the energy infrastructure, facilitating efficient long-distance electricity transmission, due to its advantages such as efficient long-distance transmission and reduced transmission losses [1]. Beyond their traditional role in efficient power transfer, HVDC systems have also played a pivotal role in addressing one of the most pressing challenges of our time: the integration of renewable energy sources into the main grid [2,3].

The Three-Level Neutral Point Clamped (NPC) Converter, a type of VSC, plays a pivotal role in HVDC systems. It excels in providing precise voltage and frequency control, ensuring grid stability during grid disturbances, and integrating renewable energy sources [4,5]. This bidirectional VSC allows for efficient power transmission in both directions, enabling the integration of renewable sources by sending excess power to the grid or balancing power flows [6]. Furthermore, the Three-Level NPC Converter offers scalability and high-voltage ratings, making it an indispensable component for modern HVDC systems aiming for flexibility, reliability, and efficiency [7].

However, these systems face a significant challenge during alternating current (AC) grid fault conditions, particularly when voltage sags occur in the power transmission lines. Voltage sags, stemming from short-circuit faults, can lead to undesirable fluctuations in the DC link voltage of converter-based HVDC systems [8,9]. Such fluctuations not only endanger the system’s stability but also have the potential to induce reversed power flow, ultimately triggering the tripping of VSC-HVDC transmission systems [10,11].

Recognizing the critical importance of ensuring the uninterrupted operation of HVDC transport systems under adverse grid conditions, this research paper introduces and investigates a novel nonlinear control technique designed to enhance the fault ride-through (FRT) capability of VSC-HVDC transmission systems during voltage sag. Furthermore, we undertake a series of semi-experimental investigations employing Processor-in-the-Loop (PIL) simulations, closely examining the system’s response to both symmetrical and asymmetrical voltage sag events, each with varying remaining voltages and durations. The proposed nonlinear control technique aims to mitigate the adverse effects of voltage sags on the operational availability of HVDC transport systems, ensuring a continuous and stable power transmission even in the face of AC grid faults.

The remainder of this paper is structured as follows: In Section 2, we present the features of the proposed HVDC system utilizing a three-level NPC, encompassing its modeling and control design. Section 3 provides an in-depth examination of the simulation results. Lastly, in Section 4, we summarize the key findings of this study and provide recommendations for future research directions.

2. Modeling and Control of VSC-HVDC

2.1. Mathematical Model of Three-Level NPC HVDC System

Figure 1 presents an equivalent system model for the point-to-point HVDC system utilizing a three-level NPC converter. This system consists of two converter stations, VSC_1 which is considered as a sending station, and VSC_2 as a receiving station. Each station connects to an AC network through resistors (R_1, R_2) and inductors (L_1, L_2), representing the impedance of the AC lines. The DC sides of the converter stations are interlinked via an HVDC cable.

The mathematical model for the converter station on the AC side of the HVDC system is presented in a synchronous reference frame (dq) as follows [12–15]:

$$\frac{di_{d1}}{dt} = -\frac{R_1}{L_1}i_{d1} + \omega_1 i_{q1} + \frac{e_{d1}}{L_1} - \frac{u_{d1}}{L_1} \tag{1a}$$

$$\frac{di_{q1}}{dt} = -\frac{R_1}{L_1}i_{q1} - \omega_1 i_{d1} + \frac{e_{q1}}{L_1} - \frac{u_{q1}}{L_1} \tag{1b}$$

$$\frac{di_{d2}}{dt} = -\frac{R_2}{L_2}i_{d2} + \omega_2 i_{q2} - \frac{e_{d2}}{L_2} + \frac{u_{d2}}{L_2} \tag{1c}$$

$$\frac{di_{q2}}{dt} = -\frac{R_2}{L_2}i_{q2} - \omega_2 i_{d2} - \frac{e_{q2}}{L_2} + \frac{u_{q2}}{L_2} \tag{1d}$$

The DC side of the HVDC system is defined by the following equations [16,17]:

$$\frac{dV_{dc1}}{dt} = \frac{e_{d1}i_{d1}}{C_1V_{dc1}} - \frac{i_c}{C_1} \tag{2a}$$

$$\frac{dV_{dc2}}{dt} = \frac{i_c}{C_1} - \frac{i_{inv}}{C_1} \tag{2b}$$

$$\frac{di_c}{dt} = -\frac{R_c}{L_c}i_c + \frac{V_{dc1} - V_{dc2}}{L_c} \tag{2c}$$

The expressions for the active and reactive powers entering both VSC1 and VSC2 can be formulated as follows [18]:

$$\begin{cases} P_i = v_{d_i}i_{d_i} + v_{q_i}i_{q_i} = v_{d_i}i_{d_i} \\ Q_i = v_{d_i}i_{q_i} + v_{q_i}i_{d_i} = v_{d_i}i_{q_i} \end{cases} \text{ with } i = 1 \text{ or } 2 \quad (3)$$

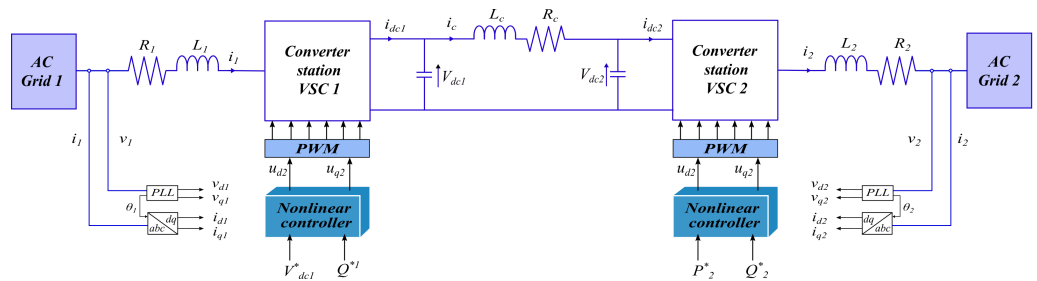


Figure 1. Topology of three-phase NPC-based HVDC transmission system.

2.2. Nonlinear Controller Design

The diagram presented in Figure 1 offers a concise overview of the VSC-HVDC system along with its corresponding control loops. Within this setup, VSC1 is assigned the crucial responsibility of regulating the DC voltage at the HVDC cable, denoted as Vdc1. On the other hand, the converter station VSC2 is dedicated to controlling active power, thereby ensuring bidirectional active power transmission. Additionally, each converter station unit independently exercises control over the reactive power, adding an extra layer of flexibility and adaptability to the overall system operation.

The controller design is developed using the Backstepping and Lyapunov approach, as presented in [19,20]. The various control laws are derived as follows:

$$u_{d1} = L_1 \left[c_1 e_1 - \frac{R_1}{L_1} i_{d1} + \omega_1 i_{q1} + \frac{e_{d1}}{L_1} - i_{d1}^* \right] \quad (4a)$$

$$u_{q1} = L_1 \left[c_2 e_2 - \frac{R_1}{L_1} i_{q1} - \omega_1 i_{d1} + \frac{e_{q1}}{L_1} \right] \quad (4b)$$

$$u_{d2} = L_2 \left[-c_3 e_3 + \frac{R_2}{L_2} i_{d2} - \omega_2 i_{q2} + \frac{e_{d2}}{L_2} + i_{d2}^* \right] \quad (4c)$$

$$u_{q2} = L_2 \left[-c_4 e_4 + \frac{R_2}{L_2} i_{q2} + \omega_2 i_{d2} + \frac{e_{q2}}{L_2} \right] \quad (4d)$$

where $c_i (i = 1, \dots, 4)$ are the controller gains and $e_i (i = 1, \dots, 4)$ are the tracking errors between the dq -currents and their reference signals.

Remark 1. In light of page constraints, we have condensed and focused our content to adhere to the allotted six pages. As a result, some detailed discussions and additional material have been omitted.

3. Simulation Results and Discussion

In order to validate the practicality and efficiency of the proposed nonlinear control strategy for a three-level NPC within an HVDC transmission system, illustrated in Figure 1, a comprehensive design and implementation process has been executed. The specifications of the implemented HVDC systems can be found in Table 1, while the relevant control parameters are given as follows: $c_1 = 700, c_2 = 1000, c_3 = 1200, c_4 = 700$. The references of outputs (V_{dc1}, Q_1, P_1 and Q_2) are chosen as: (200 KV, 0 Mvar, 100 MW, 0 Mvar) respectively. To assess the hardware implementation of the suggested control approach, a semi-experimental simulation incorporating the PIL test is performed. In this setup, real-time control signals are generated using the eZdsp F28335 Discovery board. Figure 1 illustrates the block diagram of the PIL test employed in this study. In this configuration,

the plant model is simulated within the MATLAB/Simulink environment on the host PC, while the proposed controller is executed on the eZdsp F28335 Discovery board.

Table 1. Electrical parameters of the system under consideration.

Parameters	Symbols	Values
AC voltage	V_{AC}	220 KV
Frequency	$f_{1,2}$	50 Hz
AC inductoe	$L_{1,2}$	50 mH
AC resistor	$R_{1,2}$	0.62 Ω
DC side capacitor	$C_{1,2}$	200 μ F
DC cable inductor	L_c	0.082 mH/Km
DC cable resistor	R_c	8.02 m Ω /Km

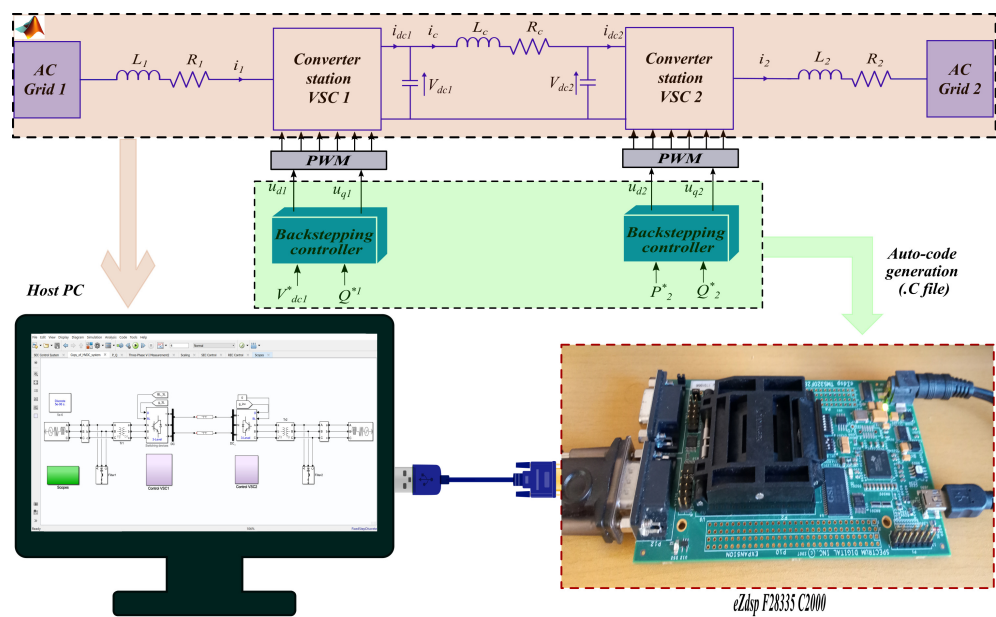


Figure 2. PIL test of the suggested approach using eZdsp F28335 Discovery board.

In this study, one case study has been performed, focusing on three-phase voltage sags occurring at the point of common coupling of Grid 2, referred to as PCC2.

In Figure 3a, we observe the voltage behavior of V_{dc1} , which clearly demonstrates its precise tracking of the specified constant reference value ($V_{dc1}^* = 200$ KV). While Figure 3b,c illustrate the temporal changes in the measured active power (P_2) and the reactive power for both sides (Q_1 and Q_2), along with their corresponding signal references. It is evident that these power values are impeccably controlled to follow their reference values.

In the case under investigation, a three-phase voltage sag takes place at the PCC2 point, causing a uniform decrease of 60% in the magnitude of three-phase voltages (v_2) within a brief time window during the voltage sag, specifically from 1 s to 1.5 s, as depicted in Figure 3g. Throughout the periods of the three-phase voltage sag that appears at PCC 2, the magnitude of the three-phase voltages (v_1) remains constant, as illustrated in Figure 3d. During the interval time [1 s, 1.5 s], we observe a reduction in the three-phase current i_1 , as shown in Figure 3e, while Figure 3h illustrates that the three-phase current i_2 remains constant. As depicted in Figure 3f,i, it's clear that throughout the voltage sag duration, the DC power for both converter stations (VSC1 and VSC2) experiences a decrease.

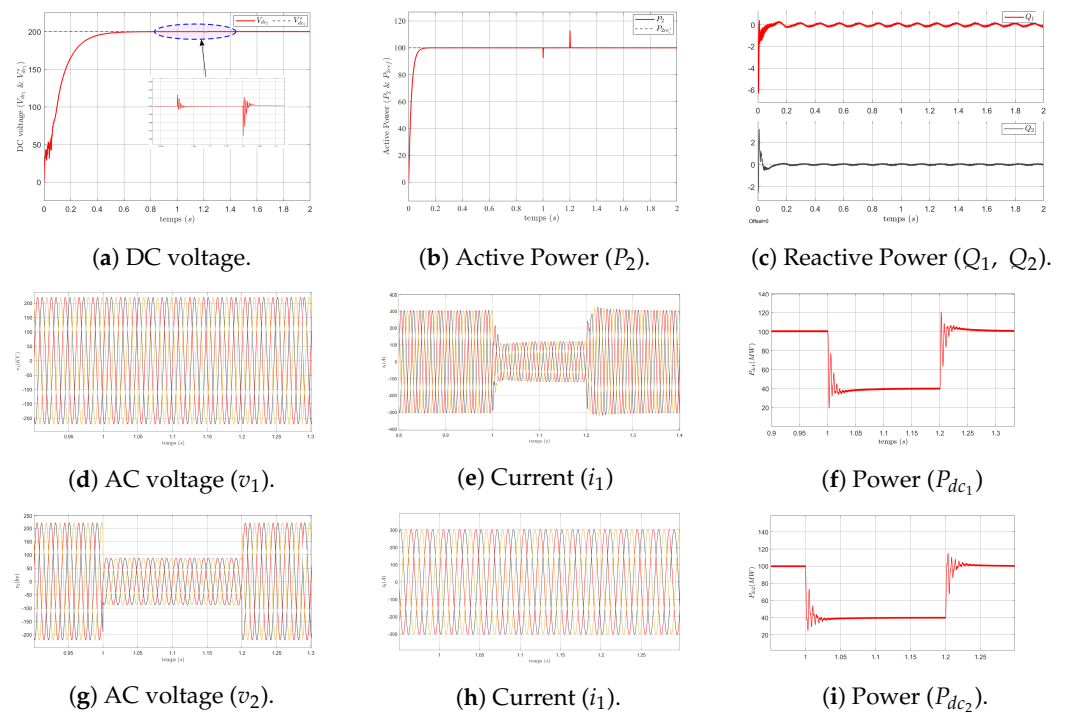


Figure 3. The performance of the proposed strategy under three-phase voltage sags.

The suggested control approach for the HVDC transmission system is aimed at maintaining power supply stability throughout the entirety of the voltage sag period, encompassing the periods before, during, and after the sag event. This signifies that the VSC-HVDC transmission system remains operational for power transmission from Grid 1 to Grid 2 even following the occurrence of a three-phase voltage sag in Grid 2.

4. Conclusions

This research paper addresses the issue of enhancing the operational availability of NPC three-level converter-based high voltage direct current (HVDC) transport systems during alternating current (AC) grid fault conditions. The objective of this paper is to develop a nonlinear control technique aimed at mitigating the impact of voltage sags on the operational availability of HVDC transport systems. To achieve this, we conducted semi-experimental investigations using Processor-in-the-loop (PIL) simulations. Through the analysis of the semi-experimental results, our aim is to gain insights into the Fault Ride-Through (FRT) capability of the VSC-HVDC transmission system. The semi-experimental results demonstrate the effectiveness of the proposed method.

Looking ahead, future work in this domain will focus on further strengthening the adaptability of the nonlinear control technique. Specifically, we will explore the development of an adaptive nonlinear control system capable of responding dynamically to varying grid conditions. Additionally, our research will transition from semi-experimental simulations to full-scale experimental setups to enhance the realism and practical applicability of our findings.

Conflicts of Interest: The authors declare no conflict of interest.

References

1. Khalid, S.; Raza, A.; Yousaf, M.Z.; Mirsaiedi, S.; Zhichu, C. Recent Advances and Future Perspectives of HVDC Development in Pakistan: A Scientometric Analysis Based Comprehensive Review. *IEEE Access* **2023**, *11*, 56408–56427. <https://doi.org/10.1109/ACCESS.2023.3283431>.
2. El Myasse, I.; Mansouri, A.; El Magri, A.; Watil, A.; Kissaoui, M.; Lajouad, R.; Ashfaq, S.; Elaadoui, N. Robust Nonlinear Control Design of MMC-HVDC Systems for Wind Power Plants Integration. In Proceedings of the 2023 3rd International Conference

- on Innovative Research in Applied Science, Engineering and Technology (IRASET), Mohammedia, Morocco, 18–19 May 2023; pp. 1–5. <https://doi.org/10.1109/IRASET57153.2023.10152899>.
3. Tian, Y.; Wickramasinghe, H.R.; Li, Z.; Pou, J.; Konstantinou, G. Review, classification and loss comparison of modular multilevel converter submodules for HVDC applications. *Energies* **2022**, *15*, 1985. <https://doi.org/https://doi.org/10.3390/en15061985>.
 4. Khan, S.; Ahmad, M.T.; Ranjan, S.; Sarwar, N. AC Fault Analysis on NPC based Multi-terminal Hybrid AC-DC system. In Proceedings of the 2023 International Conference on Recent Advances in Electrical, Electronics & Digital Healthcare Technologies (REEDCON), New Delhi, India, 1–3 May 2023; pp. 756–761. <https://doi.org/10.1109/REEDCON57544.2023.10151213>.
 5. Fan, B.; Cao, Z.; Wang, C.; Niu, Z.; Yang, C.; Wu, X. A novel neutral-point potential balance control method based on voltage feedback for neutral-point clamped three-level inverter. *Int. J. Electr. Power Energy Syst.* **2023**, *145*, 108583. <https://doi.org/https://doi.org/10.1016/j.ijepes.2022.108583>.
 6. Kim, J.Y.; Kim, H.S.; Baek, J.W.; Jeong, D.K. Analysis of effective three-level neutral point clamped converter system for the bipolar LVDC distribution. *Electronics* **2019**, *8*, 691. <https://doi.org/https://doi.org/10.3390/electronics8060691>.
 7. González-Torres, I.; Miranda-Vidales, H.; Espinoza, J.; Méndez-Barrios, C.F.; González, M. State feedback control assisted by a gain scheduling scheme for three-level NPC VSC-HVDC transmission systems. *Electr. Power Syst. Res.* **2018**, *157*, 227–237. <https://doi.org/10.1016/j.epsr.2017.12.031>.
 8. Tavakoli, S.D.; Prieto-Araujo, E.; Gomis-Bellmunt, O. AC Fault Ride Through in MMC-Based HVDC Systems. *IEEE Trans. Power Deliv.* **2022**, *37*, 2775–2786. <https://doi.org/10.1109/TPWRD.2021.3116508>.
 9. Torres, J.A.; dos Santos, R.C.; Yang, Q.; Li, J. Analyses of different approaches for detecting, classifying and locating faults in a three-terminal VSC-HVDC system. *Int. J. Electr. Power Energy Syst.* **2022**, *135*, 107514. <https://doi.org/https://doi.org/10.1016/j.ijepes.2021.107514>.
 10. Khalid, S.; Raza, A.; Alqasemi, U.; Sobahi, N.; Yousaf, M.Z.; Abbas, G.; Jamil, M. Technical assessment of hybrid HVDC circuit breaker components under M-HVDC faults. *Energies* **2021**, *14*, 8148. <https://doi.org/https://doi.org/10.3390/en14238148>.
 11. Li, X.; Xu, Z.; Zhang, Z. Enhanced Ride-Through Capability Under Rectifier-Side AC Fault for Series LCC-MMC Hybrid HVDC System. *IEEE Access* **2021**, *9*, 153050–153057. <https://doi.org/10.1109/ACCESS.2021.3127717>.
 12. El Magri, A.; Giri, F.; Besancon, G.; El Fadili, A.; Dugard, L.; Chaoui, F.Z. Sensorless adaptive output feedback control of wind energy systems with PMS generators. *Control Eng. Pract.* **2013**, *21*, 530–543. <https://doi.org/https://doi.org/10.1016/j.conengprac.2012.11.005>.
 13. Pouresmaeil, E.; Montesinos-Miracle, D.; Gomis-Bellmunt, O. Control Scheme of Three-Level NPC Inverter for Integration of Renewable Energy Resources Into AC Grid. *IEEE Syst. J.* **2012**, *6*, 242–253. <https://doi.org/10.1109/JSYST.2011.2162922>.
 14. Saini, D.K.; Khan, S.; Bhowmick, S. Modelling of neutral point clamped based VSC-HVDC system. In Proceedings of the 2016 IEEE 7th Power India International Conference (PIICON), Bikaner, India, 25–27 November 2016; pp. 1–6. <https://doi.org/10.1109/POWERI.2016.8077217>.
 15. Watil, A.; El Magri, A.; Raihani, A.; Lajouad, R.; Giri, F. An adaptive nonlinear observer for sensorless wind energy conversion system with PMSG. *Control Eng. Pract.* **2020**, *98*, 104356. <https://doi.org/https://doi.org/10.1016/j.conengprac.2020.104356>.
 16. EL MYASSE, I.; EL MAGRI, A.; KISSAOUI, M.; LAJOUAD, R.; WATIL, A.; BERRAHAL, C. Adaptive Nonlinear Control of Generator Load VSC-HVDC Association. *IFAC-PapersOnLine* **2022**, *55*, 782–787. <https://doi.org/https://doi.org/10.1016/j.ifacol.2022.07.408>.
 17. Mansouri, A.; El Magri, A.; Lajouad, R.; Giri, F.; Watil, A. Optimization Strategies and Nonlinear Control for Hybrid Renewable Energy Conversion System. *Int. J. Control Autom. Syst.* **2023**, 1–8. <https://doi.org/https://doi.org/10.1007/s12555-023-0058-7>.
 18. Mansouri, A.; Myasse, I.e.; Magri, A.E.; Lajouad, R.; Giri, F. Nonlinear Control of Five-Phase PMSG Wind Turbine connected to Vienna Type Rectifier Using SVPWM. In Proceedings of the 2023 3rd International Conference on Innovative Research in Applied Science, Engineering and Technology (IRASET), Mohammedia, Morocco, 18–19 May 2023; pp. 1–6. <https://doi.org/10.1109/IRASET57153.2023.10152932>.
 19. El Mezdi, K.; El Magri, A.; Watil, A.; El Myasse, I.; Bahatti, L.; Lajouad, R.; Ouabi, H. Nonlinear control design and stability analysis of hybrid grid-connected photovoltaic-Battery energy storage system with ANN-MPPT method. *J. Energy Storage* **2023**, *72*, 108747. <https://doi.org/https://doi.org/10.1016/j.est.2023.108747>.
 20. El Myasse, I.; El Magri, A.; Kissaoui, M.; Lajouad, R.; Giri, F.; Watil, A.; Bahatti, L. Observer and Nonlinear Control Design of VSC-HVDC Transmission System. *Int. J. Electr. Power Energy Syst.* **2023**, *145*, 108609. <https://doi.org/https://doi.org/10.1016/j.ijepes.2022.108609>.

Disclaimer/Publisher’s Note: The statements, opinions and data contained in all publications are solely those of the individual author(s) and contributor(s) and not of MDPI and/or the editor(s). MDPI and/or the editor(s) disclaim responsibility for any injury to people or property resulting from any ideas, methods, instructions or products referred to in the content.